Electric Field Effects on Aromatic and Aliphatic Hydrocarbons: A Density-Functional Study

ARTICLE *in* THE JOURNAL OF PHYSICAL CHEMISTRY A · OCTOBER 2007

Impact Factor: 2.69 · DOI: 10.1021/jp074051v · Source: PubMed

Electric Field Effects on Aromatic and Aliphatic Hydrocarbons: A Density-Functional Study

Dhurba Rai,[†] Harshad Joshi,[†,‡] Anant D. Kulkarni,*[,§,||] Shridhar P. Gejji,[§] and Rajeev K. Pathak[†,⊥]

Department of Physics, University of Pune, Pune-411007, India, Department of Chemistry, University of Pune, Pune-411007, India, and Department of Physics, Tulane University, New Orleans, Louisiana 70118

Received: May 25, 2007; In Final Form: July 12, 2007

The influence of a uniform static external electric field on some aliphatic and aromatic molecular species is studied within the density functional theory (DFT) employing the 6-311++G(2d,2p) basis set with B3LYP exchange-correlation prescription. The electric field perturbs the molecular geometry but drastically alters the dipole moments and engenders, to a varying degree, the molecular vibrational Stark effect, i.e., shifts in the infrared (IR) vibrational frequencies accompanied by spectral intensity redistribution. For polar molecules, significant negative ("red") and positive ("blue") frequency shifts are observed for field orientations both parallel and antiparallel to their permanent dipole moments. Further, a selective reordering of frontier orbitals is observed to be brought about by moderately intense fields. In particular, molecules having a lowest unoccupied molecular orbital (LUMO) with predominant π character possess a threshold field beyond which energy gap between the highest occupied molecular orbital (HOMO) and LUMO diminishes rapidly. A time-dependent (TD) DFT analysis reveals that an increase in the applied field strength by and large increases the excitation energies corresponding to significant electronic transitions among frontier MOs with a concomitant decrease in their oscillator strengths.

I. Introduction

With the advent of molecular electronics, recent years have witnessed a remarkable progress on the understanding of current conduction through prototype molecular electronic devices such as a single or, at best, a countable number of molecules.[1,3,4] The conductance spectra of molecules and molecular wires have a direct bearing on their response to applied external electric fields.[1−4] Electric fields modify the molecular geometry, drastically alter the electric dipole moments, and bring out a redistribution of molecular orbitals (MOs) as well as a reduction in the energy gap between frontier molecular orbitals. Further, appreciable shifts in their infrared (IR) vibrational spectra accompanied by a redistribution of the corresponding spectral intensities as a function of the field strength are observed, an effect that is aptly termed the molecular vibrational stark effect (VSE). Choi et al.[1] studied the role of molecular orbitals in the conductance spectra of benzene using the hybrid density functional calculations employing the 6-311++G(d,p) basis set. A set of threshold electric fields was observed beyond which the energy of the LUMO + 2 gets lowered below the energy of LUMO (lowest unoccupied molecular orbital) rendering the molecule electronically active ($F^{th}_{||} = 0.2$ V/Å and $F^{th}_{\perp} = 0.7$ V/Å, where $F^{th}_{||}$ and $F^{th}_{\perp}$ denote the threshold electric field strengths of the external electric field $\vec{F}$ applied parallel and perpendicular to the aromatic plane, respectively). More recently, Li et al.[2] found an appreciable reduction of the HOMO−LUMO gap on increasing the length of molecular chain constituting the molecular wires. Diminishing the gap is also evinced with increasing external electric field strengths leading to spatial distributions of frontier molecular orbitals that vary from fully delocalized form to partly localized. Electrical conduction through molecules essentially requires "promoting" an electron to erstwhile virtual, unoccupied molecular orbitals (UMOs). Contribution to the current conduction from higher UMOs and the lower occupied ones has been investigated by Wang, Fu, and Luo.[4] On the basis of their studies on benzene-1,4-dithiol and α,α'-xylyldithiol, they inferred that the upper UMOs (LUMO + *n*, where n = 10, 11, 12, 13, ...) contributed significantly to the electron conduction compared to the low-lying ones. Within the density functional theory (DFT), Tóbik et al.[5] investigated the changes in the electronic structure of small slabs of benzene (six layers) and anthracene (four layers) due to electric field applied perpendicular to the slabs. They found that the HOMO−LUMO band gap in benzene and anthracene slabs "closed down" at the field values of 0.005 and 0.014 au, respectively (1 au of electric field strength ≅ 51.42 V/Å). All these foregoing features form important descriptors in molecular electronic architecture with molecular wire elements[6] and in modeling the electrical characteristics of molecular devices.[7] A property of any molecule that is of primal importance in the description of its response to an external electric field is its electric polarizability, α_{ij}, and higher order polarizabilities. These electrical properties enter in the expansion

* To whom correspondence should be addressed. E-mail: anantkul@chem.unipune.ernet.in, anantkul@dcci.unipi.it.
† Department of Physics, University of Pune.
‡ Present address: Max Planck Institute for Biophysical Chemistry, Am Fassberg 11 D- 37077 Göttingen, Germany.
§ Department of Chemistry, University of Pune.
|| Present address: Dipartimento di Chimica e Chimica Industriale, Universita di Pisa, Via Risorgimento 35, 56126 Pisa, Italy.
⊥ Department of Physics, Tulane University.

10.1021/jp074051v CCC: $37.00
Published on Web 08/28/2007

TABLE 1: Aliphatic Molecules: Variation in Bond Lengths (Parallel to the Applied Field) and Electric Dipole Moments of Molecules at Various Field Strengths[a]

	CH_4		CH_3F		HCHO		C_2H_4		C_2H_2			
field (au)[b]	C−H (Å)	[μ] (D)	C−F (Å)	[μ] (D)	C−O (Å)	[μ] (D)	C−C (Å)	[μ] (D)	C−H (Å)	(C−C) (Å)	(C−H) (Å)	[μ] (D)
0.040	1.093	[1.66]	1.491	[4.18]	1.231	[4.82]	1.337	[3.79]	1.059	(1.204)	(1.081)	[3.30]
0.030	1.089	[1.21]	1.458	[3.55]	1.222	[4.20]	1.332	[2.77]	1.058	(1.200)	(1.075)	[2.43]
0.020	1.087	[0.80]	1.433	[2.99]	1.214	[3.60]	1.328	[1.82]	1.059	(1.198)	(1.069)	[1.60]
0.010	1.087	[0.40]	1.412	[2.46]	1.207	[3.01]	1.326	[0.90]	1.059	(1.197)	(1.065)	[0.79]
0.005	1.087	[0.20]	1.403	[2.20]	1.204	[2.71]	1.326	[0.45]	1.061	(1.196)	(1.062)	[0.39]
0	1.088	[0.00]	1.395	[1.96]	1.201	[2.42]	1.326	[0.00]	1.061	(1.196)	(1.061)	[0.00]
−0.005	1.089	[−0.20]	1.387	[1.71]	1.198	[2.12]						
−0.010	1.091	[−0.40]	1.380	[1.47]	1.195	[1.82]						
−0.020	1.095	[−0.83]	1.366	[0.97]	1.189	[1.20]						
−0.030	1.101	[−1.29]	1.353	[0.48]	1.184	[0.53]						
−0.035	1.105	[−1.54]	1.348	[0.23]	1.181	[0.17]						
−0.040	1.109	[−1.81]	1.342	[−0.01]	1.179	[−0.22]						
−0.045			1.337	[−0.27]	1.176	[−0.67]						
−0.050			1.332	[−0.53]	1.174	[−1.19]						

[a] In polar molecules, the fields are applied in the directions of permanent dipole moments. In methane, the field is applied from C to H and in acetylene from the C−H bond in the first position to the latter. For polar species, the positive values represent the fields oriented parallel to the permanent dipole moment, while the negative ones represent antiparallel orientations. Also cf. ref 13 for variation of bond lengths and dipole moments of methane and acetylene as a function of applied field. [b] 1 atomic unit of electric field = 51.42 V/Å = 5142 MV/cm = 5.142×10^{11} V/m (SI).

of the total energy[8] as a function of the external electric field $\vec{F}$ via

$$E = E^{o} - \mu_i F_i - \frac{1}{2}\alpha_{ij}F_iF_j - \frac{1}{6}\beta_{ijk}F_iF_jF_k - \frac{1}{24}\gamma_{ijkl}F_iF_jF_kF_l - \cdots \quad (1)$$

where summation over repeated indices is assumed. E^{o} is the energy of molecule in absence of field, the F_i's ($i = 1-3$) denote the components of applied field, the μ_i's denote the components of the electric dipole moment, and β_{ijk} and γ_{ijkl} are the components of first- and second-order hyperpolarizabilities, respectively. Here, the molecular electric dipole moment $\vec{\mu}$ is defined as per the usual convention,

$$\vec{\mu} = \int \vec{r}\,\rho(\vec{r})\,d\tau$$

where $\rho(\vec{r})$ is the charge density at the location $\vec{r}$. The net dipole moment, the most significant parameter that couples with the externally applied field, arises as a sum-total contribution of various response terms:

$$\mu_i = \mu_i^{o} + \alpha_{ij}F_j + \frac{1}{2}\beta_{ijk}F_jF_k + \frac{1}{6}\gamma_{ijkl}F_jF_kF_l + \cdots \quad (2)$$

Here μ_i^{o} denotes the i^{th} component of permanent dipole moment in the *absence* of the field. The polarizability, α_{ij}, thus quantifies the linear response of molecule to the applied field while β_{ijk} and γ_{ijkl} describe the leading nonlinear responses. The electrical polarizabilities in general comprise electronic, vibrational, and rotational contributions. The vibrational contribution to the electrical properties have components arising from vibrational average (which also incorporates the zero point contribution) of the electronic properties over the perturbed vibrational wave function and interaction of the nuclei with the applied field.[9] The latter influences the structure and shifts the vibrational levels, consequently, the vibrational (IR) spectrum of the molecule. This is commonly referred to as the vibrational stark effect (VSE)[10,11] and is quantified by a parameter viz. the Stark tuning rate (STR), defined to be the shift in vibrational frequency/unit applied electric field strength. The shift in the vibrational (angular) frequency in terms of electric field[11] is expressible as

$$\Delta\omega = -\frac{1}{\hbar}\left[\Delta\mu_i F_i + \frac{1}{2}\Delta\alpha_{ij}F_iF_j + \cdots\right] \quad (3)$$

where $\Delta\mu_i$ and $\Delta\alpha_{ij}$ are the differences in the dipole moments and the linear polarizabilities corresponding to the ground and excited states. Shift in vibrational frequency due to electric fields in free and chemisorbed molecules has been investigated at different levels of theory by various groups.[12,14] VSE has also been experimentally tractable[15,16] through vibrational frequency shifts and redistribution of spectral line intensities of the IR vibrational spectra. In VSE spectroscopy, these shifts provide information on the different modes of molecular vibration, including the understanding of anharmonicity.[11,17] Furthermore, STR directly yields a map of variation in local fields at a specific site in a molecular system. Thus, deviations in the vibrational (IR) spectrum brought about by electric fields from their field-free counterparts offer an alternative tool for probing the electrostatic environment at dedicated sites of molecular complexes.[18]

The spirit underlying this work is to explore some generic responses of certain selected molecular species when stimulated by external uniform electric fields. We attempt a systematic theoretical study on the geometry, electronic states, and the vibrational Stark effect. The diversified set of molecules studied herein comprises methane, fluoromethane, ethylene, acetylene, and formaldehyde (aliphatic species), as well as benzene, fluorobenzene, chlorobenzene, 1,4-chlorofluorobenzene, hexafluorobenzene, and pyridine (aromatic species). A molecule possessing a dipole moment (either intrinsic or field-induced) tends to align its dipole moment in the direction of applied field. Hence it is expected that the results obtained in the present gas-phase calculation in the presence of the electric field would reasonably represent the experimental or computational results obtained by matrix isolation[19,20] of the molecules in a similar environment.

In the following section we outline the methodology adopted in this endeavor, followed by a discussion on the changes in certain salient properties along with their ramifications.

TABLE 2: Aromatic Molecules: Bond Lengths Collinear with the Applied Field and the Electric Dipole Moments of Molecules at Various Field Strengths[a]

	C_6H_6			C_6H_5F			C_6H_5Cl			1,4-C_6H_4ClF			C_6F_6			C_5H_5N		
field (au)[b]	C−H (Å)	(C−C) (Å)	(C−H) (Å)	[μ] (D)	C−F (Å)	(C−C) (Å)	(C−H) (Å)	[μ] (D)	Cl−C (Å)	(C−C) (Å)	(C−H) (Å)	[μ] (D)	Cl−C (Å)	(C−C) (Å)	(C−F) (Å)	[μ] (D)	C−F (Å)	(C−C) (Å)	(C−F) (Å)	[μ] (D)	∠(HNH) (deg)	(C−H) (Å)	[μ] (D)
0.040					1.483	(1.40 6)	(1.089)	[11.07][c]									1.414	(1.396)	(1.281)	[10.33]	114.64	(1.089)	[10.38]
0.030	1.095	(1. 39 6)	(1. 08 4)	[6. 36][a]	1.436	(1.400)	(1.084)	[8.45]	1.892	(1.401)	(1.085)	[11.28]	1.8 72	(1.393)	(1. 29 9)	[10.06]	1.388	(1.393)	(1.292)	[7.59]	115.29	(1.085)	[8.10]
0.020	1.088	(1. 39 4)	(1. 08 2)	[4. 13]	1.402	(1.396)	(1.081)	[6.09]	1.822	(1.396)	(1.082)	[7.77]	1.8 14	(1. 39 1)	(1. 31 5)	[6.47]	1.367	(1.390)	(1.305)	[5.00]	115.99	(1.082)	[6.07]
0.010	1.084	(1. 39 2)	(1. 08 1)	[2. 04]	1.376	(1.393)	(1.080)	[3.84]	1.785	(1. 39 3)	(1.080)	[4.73]	1.7 81)	(1. 39 0)	(1. 33 3	[3.25]	1.348	(1.389)	(1.319)	[2.47]	116.70	(1.081)	[4.16]
0.005	1.083	(1. 39 2)	(1. 08 1)	[1. 01]	1.365	(1.393)	(1.080)	[2.73]	1.771	(1.392)	(1.08 0)	[3.27]	1.7 67	(1. 39 0)	(1. 34 3)	[1.69]	1.340	(1.389)	(1.326)	[1.22]	117.03	(1.081)	[3.22]
0	1.082	(1. 39 2)	(1. 08 2)	[0. 00]	1.355	(1.392)	(1.081)	[1.62]	1.759	(1.391)	(1.08 1)	[1.81]	1.7 57	(1. 39 0)	(1. 35 2)	[0.15]	1.333	(1.389)	(1.333)	[0.00]	117.34	(1.082)	[2.30]
−0.005					1.345	(1.391)	(1.082)	[0.51]	1.749	(1.391)	(1.08 2)	[0.36]	1.7 48	(1. 39 1)	(1. 36 2)	[−1.37]					117.58	(1.082)	[1.37]
−0.010					1.336	(1.391)	(1.083)	[−0.60]	1.739	(1.390)	(1.083)	[−1.12]	1.7 38	(1. 39 1)	(1. 37 5)	[−2.93]					117.95	(1.084)	[−0.44]
−0.020					1.319	(1.390)	(1.087)	[−2.91]	1.720	(1.390)	(1.08 7)	[−4.21]	1.721	(1. 39 3)	(1. 40 2)	[−6.12]					118.52	(1.088)	[−1.44]
−0.030					1.304	(1.390)	(1.094)	[−5.39][c]					1.705	(1. 39 5)	(1. 43 6)	[−9.54]					121.24	(1.104)	[−8.29]

[a] In polar molecules, fields are applied along the permanent dipole moments. In benzene (hexafluorobenzene), the field is applied from the C−H (C−F) bond in the first position to the latter. [b] 1 atomic unit of electric field = 51.42 V/Å = 5142 mV/cm = 5.142×10^{11} V/m (SI). [c] Value corresponding to a transition state-like structure, characterized by 1 imaginary frequency.

Figure 1. Orientation of field applied to benzene and the alignment of induced dipole moment illustrated.

II. Methodology

We employ the Gaussian-03 suite of programs[21] to investigate the structural and electronic changes brought about by the applied uniform static electric fields, such as those produced by uniform, equal but oppositely charged plates of an infinite parallel-plate capacitor. Systematic study on various modifications under the influence of externally imposed field is carried out within the premise of the density functional theory (DFT) using Becke's three-parameter hybrid functional[24] (B3) combined with the electron-correlation functional of Lee, Yang, and Parr[25] (LYP). All calculations were carried out by optimizing the geometry using the 6-311++G(2d,2p) basis set (triple-ζ basis set augmented with diffuse and polarization functions), which uses 27 basis functions for heavy atoms and 10 for the hydrogen atoms. By virtue of the flexibility proffered by the polarization and diffuse functions, such an extended basis set is deemed crucial for adapting to an external electric field. Actually at a given location, the sum-total electric field will be nonuniform owing to the contribution from local molecular environment. The molecular geometry optimizations carried out herein include, self-consistently, both the effects of the applied field and the local one. Here the external electric field employed is a uniform, bipolar one by means of which we investigate the general trends in the molecular properties. The applied fields were made to orient along (positive) and opposite (negative) to permanent or induced dipole moments of polar as well as nonpolar aromatic and aliphatic hydrocarbons and also perpendicular to the of the molecular "plane" wherever pertinent. The field was increased gradually from zero until it either dissociated the molecules or escalated the molecules to a transition state-like (TS) structure, so termed for being characterized by a single imaginary frequency, hence a first-order saddle point on the potential energy surface. We have considered fields of magnitude $\sim 10^{-3}$—$\sim 10^{-2}$ au, which can be observed in zeolite[26] or protein cavities.[18,27] Throughout this work, we use atomic units for field strengths (recall that 1 au of electric field $\cong$ 51.42 V/Å). Further, we have subscribed to the Stark tuning rates in the units of cm^{-1}/(MV/cm), as is customary.[16,29] Computations of vibrational frequencies were carried out in presence of field to confirm local minimality of the optimized structures in field,- and to yield the IR spectrum perturbed by the applied field. Since the optimization and the frequency calculations were carried out in the presence of field, the effect of geometry changes upon electric field application is well incorporated in VSE. The time-independent calculation assumes a uniform spatially and temporally *constant* electric field that extends to infinity is *always* present. This could be accomplished by placing the molecule in a parallel-plate capacitor whose plates are of infinite extent and well-separated so that the molecular wave functions all have negligible values at the boundaries (at the plates), thus eliminating boundary problems.

TABLE 3: Diagonal Components of Molecular Polarizability of Benzene and Fluorobenzene Corresponding to the Geometry Optimized at B3LYP/6-311++G(2d,2p)[a]

	benzene			fluorobenzene		
field (au)	α_{xx} (au)	α_{yy} (au)	α_{zz} (au)	α_{xx} (au)	α_{yy} (au)	α_{zz} (au)
0.040[c]				84.14	92.83	44.20
0.030[b]	82.26	90.43	50.93	81.35	83.50	42.76
0.020	80.85	83.05	44.89	80.00	81.38	42.07
0.010	80.05	80.53	43.82	79.28	80.75	41.96
0.005	79.93	80.12	43.53	79.12	81.00	42.30
0	79.80	79.80	43.35	79.09	81.65	42.30
−0.005				79.21	82.60	42.57
−0.010				79.19	83.85	43.46
−0.200				80.07	87.81	45.00
−0.030[c]				81.42	96.33	126.59

[a] Field is applied in the direction shown in Figure 1. The 10H in that figure is replaced by a fluorine atom for fluorobenzene geometry. 1 au of electric polarizabillity $\approx 4.94 \times 10^{-10}$ D/(V/cm). [b] [c]This field strength escalates benzene (fluorobenzene) to a transition state structure. See ref 28 and the references therein for the comparison of field-free components of polarizability of benzene calculated at the B3LYP/6-311++G(2d,2p) level of theory with the other various methods.

TABLE 4: Vibrational Frequency, IR Intensity, and Frequency Shifts Corresponding to CF Stretching in Fluoromethane at Various Fields Applied along Its Permanent Dipole Moment

field (au)	ν_{CF} (cm^{-1})	intensity ($km \cdot mol^{-1}$)	$\Delta\nu_{CF}$ (cm^{-1})
0.040	763	189	−267
0.030	855	164	−175
0.020	925	144	−105
0.010	982	126	−48
0.005	1009	119	−21
0	1030	112	0
−0.005	1051	105	21
−0.010	1067	99	37
−0.020	1103	89	73
−0.030	1131	79	101
−0.040	1154	70	124

Recently, in an extensive review, Dreuw and Head-Gordon[30] advocated that the time-dependent DFT has emerged as a reliable and prominent method to study the excited-state properties of medium- and large-sized molecular systems. Also, Burke and co-workers[30] reported detailed studies on time-dependent version of DFT (TD−DFT). To delve into the nature of frontier HOMO−LUMO transitions, we have calculated TD−DFT-based excitation energies and the oscillator strengths yielded by employing the 6-311++G(2d,2p) basis set. The computations performed being essentially perturbative in nature, numerically large field strengths have been summarily avoided. Since the investigations on field effects have been carried out on isolated molecular species, a direct comparison of the calculated quantities with the other correlated ab initio calculations or with the experiments is rather elusive. The field-free values or the values obtained under similar environment as in this work are compared with the available molecular data.

III. Results and Discussion

1. Geometry and Electric Dipole Moments. We have considered some selected aliphatic and aromatic molecules belonging to different symmetry point groups. In aliphatic polar species, viz., fluoromethane and formaldehyde, the fields were applied parallel to their permanent dipole moments, whereas, in nonpolar species, viz., methane, ethylene and acetylene, they were made to orient along the symmetry axes C_3, C_2, and C_∞, respectively. The changes in the bond lengths and dipole moments of single aliphatic molecules are summarized in Table 1. Although a direct comparison of the present results with other methods or experimental values is not possible, the trends in the variation of some quantities (e.g., dipole moments, bond lengths, etc.) as a function of applied field can be corroborated with the available literature, e.g., for CH_4 reported by Duran, Andrés, Lledós, and Bertrán[12] within the framework of the Hartree−Fock (HF) theory. It is evident from the table that the C−F bond in fluoromethane somewhat elongates for parallel fields while it shortens for antiparallel ones. Variations in bond lengths and the dipole moments of methane and acetylene with applied field are in good accord with those reported by Masunov et al.[13] at the HF/D95** level of theory. For methane, the C−H bond lengths are seen to elongate, albeit slightly, for both the orientations of the field. For the polar aliphatic molecules discussed herein, the external dipole moment variation ranges over a factor of +2 through −1/2. Despite relatively small variations in the nuclear skeleton, these drastic variations in the dipole moment point out to appreciable shifts in the center of *negative* charge density, i.e., the electron density. This is a simple consequence of the agility of the electron cloud (over the nuclei) to adjust to external

TABLE 5: Vibrational Frequencies, IR Intensities, and the Frequency Shifts Corresponding to CF and CH (Located Diametrically Opposite to CF Bond) Stretching in Fluorobenzene at Various Fields Applied along the Permanent Dipole Moment[a]

field (au)	ν_{CF} (cm^{-1})	intens ($km \cdot mol^{-1}$)	$\Delta\nu_{CF}$ (cm^{-1})	ν'_{CH} (cm^{-1})	intens ($km \cdot mo\ l^{-1}$)	ν''_{CH} (cm^{-1})	intens ($km \cdot mol^{-1}$)	ν'''_{CH} (cm^{-1})	intens ($km \cdot mol^{-1}$)
0.040[b]	1052	13	−185	3129	158	3140	14	3183	44
0.030	1093	62	−144	3158	38	3176	22	3198	29
0.020	1139	89	−98	3176	19	3194	0	3208	15
0.010	1205	61	−32	3184	7	3197	2	3212	2
0.005	1221	90	−16	3182	2	3199	6	3209	0
0	1237	105	0	3175	0	3196	14	3208	0
−0.005	1253	115	16	3163	2	3188	26	3209	0
−0.010	1269	121	32	3146	12	3177	38	3209	2
−0.020	1298	126	61	3091	70	3153	57	3207	4
−0.030[b]	1323	128	86	3002	206	3122	83	3199	19

[a] Three distinct vibrational modes are involved in CH stretching. [b] This field strength takes the molecule to a transition state.

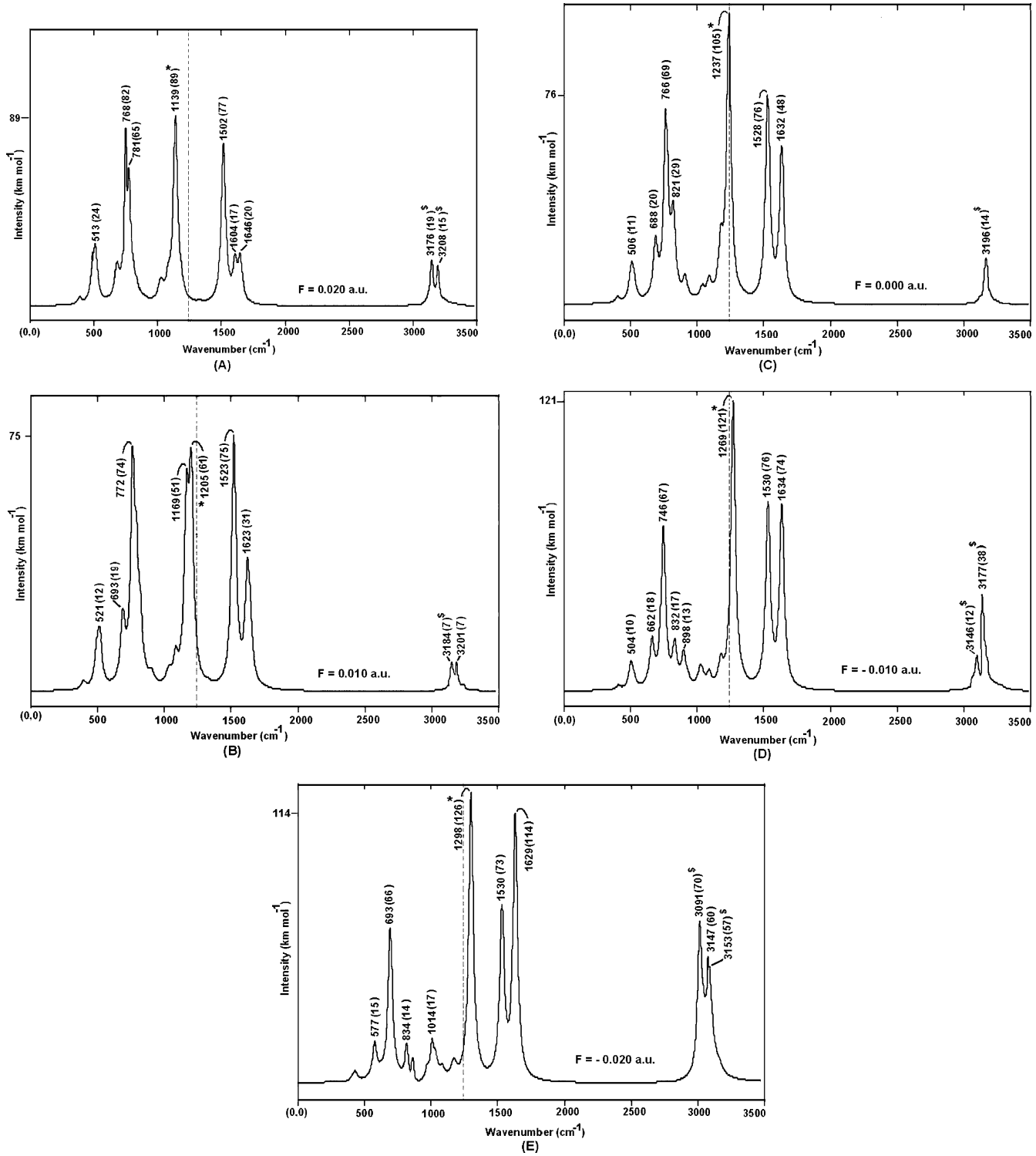

Figure 2. (A, B) Molecular vibrational Stark effect: IR spectrum of fluorobenzene at applied field strength, $F = 0.020$ and $+0.010$ au, respectively. Asterisk indicated a frequency corresponding to CF stretching as a function of applied uniform external electric field (in au) parallel (positive) and antiparallel (negative) to the permanent dipole moment. "$" indicates frequency corresponding to CH (bond, diametrically opposite to CF) stretching. Vertical dotted line represents the field free position of F−C stretching frequency. (C, D) Molecular vibrational Stark effect: IR spectrum of fluorobenzene at applied field strength, $F = 0.000$ and -0.010 au, respectively. (E) Molecular vibrational Stark effect: IR spectrum of fluorobenzene at applied field strength, $F = -0.020$ au.

stimuli. As there is a tendency for preponderance of electron density toward the positive "capacitor plate", the positive and negative fields tend to align the dipole moments along the respective field directions. Polar molecules subject to negative fields, however, must offset the "field-free" dipole moment before their dipole moment aligns with the applied field. The nonpolar aliphatic hydrocarbons methane, ethylene, and acetylene with the applied fields oriented along one of the C−H bonds, C═C, and C≡C, respectively, show comparatively a slower variation in the dipole moments and the bond lengths as is also evident from Table 1. The almost linear variation of the dipole moment over the given ranges of parallel and antiparallel fields is evident from the data presented in Tables 1 and 2.

TABLE 6: Vibrational Frequencies, IR Intensities, and Frequency Shifts of Cl−C and C−F Stretching in 1,4-Chlorofluorobenzene at Various Fields Applied along the Permanent Dipole Moment

field (au)	ν_{CF} (cm^{-1})	intens ($km \cdot mol^{-1}$)	$\Delta\nu_{CF}$ (cm^{-1})	ν_{ClC} (cm^{-1})	intens ($km \cdot mol^{-1}$)	$\Delta\nu_{ClC}$ (cm^{-1})
0.030	1328	128	85	1042	2	−54
0.020	1306	137	63	1057	12	−39
0.010	1276	135	33	1078	33	−18
0.005	1259	130	16	1088	44	−8
0	1243	121	0	1096	55	0
−0.005	1227	110	−16	1103	67	7
−0.010	1208	86	−35	1109	82	13
−0.020	1144	49	−99	1115	126	19
−0.030	1095	101	−148	1118	84	22

Aromatic molecules also exhibit their characteristic responses. Owing to its D_{6h} symmetry, benzene, although devoid of a permanent electric dipole moment, acquires an induced moment in the presence of an external electric field, which aligns the molecule in the direction of applied field. Changes in the bond lengths caused by the field applied along a C−H bond (cf. Figure 1) are summarized in Table 2. From this table, it is evident that the distortion caused in the geometry is negligible, but owing to the π-electron cloud, the induced dipole moment is seen to acquire an appreciable value of 4.13 D at a field strength of +0.020 au with the planarity of the molecule is still maintained. Although also conforming to the D_{6h} symmetry, hexafluorobenzene has an enhanced electron density around the fluorine atoms, as opposed to the case in benzene where C is more electronegative than H. Contribution to the electron density due to lone pairs on the F atoms in hexafluorobenzene induces a characteristic response when subject to an external electric field. The field-induced distortions in geometry are appreciable, so as the dipole moment changes for both parallel and antiparallel (to $\vec{\mu}$) field orientations. To investigate the effect of field on molecules with lesser symmetry, we have studied fluorobenzene, chlorobenzene, and 1,4-chlorofluorobenzene and pyridine that has a high permanent intrinsic (field-free) dipole moment. Marked variations in the dipole moment from its zero field value would be evident from Table 2. For the polar aromatic species studied herein, the dipole moments range 2 orders of magnitude both for positive and negatively oriented fields, as is evidenced for 1,4-chlorofluorobenzene. Here, the delocalized π-electrons are responsible for considerable changes in dipole moments. The almost linear variation of the dipole moment (in D) with both positive and negative applied fields is remarkable, as is typified for fluorobenzene: $\mu \sim \{234.01F$ (au) + 1.51$\}$ D. Diagonal components of the net molecular polarizability of benzene and fluorobenzene are presented in Table 3, showing some appreciable variation in α_{yy}, e.g., for both positive and negative fields, applied along the *y*-axis. The field-free components of polarizability of benzene are somewhat lesser than those calculated by density-functional perturbation theory with a generalized gradient approximation prescription;[28] however, the qualitative *trends* in the response evoked by the external electric field remain the same.

2. Vibrational Stark Effect. The effect of field on the frequency and intensity of C−F vibration in fluoromethane is presented in Table 4. As is readily inferred from the table, a "red" shift of 104 cm^{-1} in C−F stretching vibration is observed when field of magnitude 0.020 au is applied along the permanent dipole moment. This is in accord with the lengthening of C−F bond (cf. Table 1) under the influence of applied field. Vibrational frequencies of the C−F and the opposite C−H bond stretches in fluorobenzene at various field strengths are presented in Table 5. Figure 2 illustrates the infrared spectra for fluorobenzene. A red (blue) shift of 98 (61) cm^{-1} in C−F stretching is found when field of magnitude 0.020 au is applied along (opposite) the permanent dipole moment. Once again, these shifts may be attributed to the elongation and contraction of the C−F bond (cf. Table 2). A fit of ν (cm^{-1}) versus the applied field (MV/cm) yields two different slopes for positive field (slope = 0.93 cm^{-1}/(MV/cm)) and the negative one (slope = 0.54 cm^{-1}/(MV/cm)), representing STR by the mean value of 0.73 cm^{-1}/(MV/cm), for C−F stretching corresponding to the frequency shifts spanning the range −144 through +61 cm^{-1}. This mean STR underestimates the experimental value 0.84 cm^{-1}/(MV/cm)[29] by about 13%, but rhymes with the latter at least in order of magnitude. Further, as deduced from the table, the C−H bond stretching actually involves three distinct but rather closely spaced fundamental modes of vibration. For the field-free case, however, the intensities corresponding to two of these modes are too insignificant to be observed. On the other hand, in the presence of the field as depicted in the Figure 2, only two of these three modes are perceived, as the intensity associated with the central mode is not that pronounced, for the forward field, while the reverse field leads to a diminishingly insignificant intensity for the last mode. As expected, shifts in C−H stretching intensities are not pronounced as in C−F, as the C−H stretches get distributed among three distinct modes. The carbon−halogen vibrational modes for 1,4-chlorofluorobenzene exhibit a peculiar redistribution of frequencies and intensities, as presented in Table 6. Increasing field in the direction of the dipole moment (Cl → C) enhances frequencies and intensities for the C−F stretch, exactly opposed to the case of C−Cl. Reversal of the field enhances the C−Cl frequency and diminishes that for C−F. However, interestingly, there is a complementarity in the intensity profile for these two stretches: where the C−F intensity has a minimum, the C−Cl

TABLE 7: Crossing of Higher Unoccupied MO Energy Levels with LUMO beyond Which HOMO−LUMO Energy Gap (Δ_{HL}) Decreases Rapidly and the Threshold Fields (F^{th}) at Which Crossing Occurs[a]

		threshold fields		
molecules	crossing of LUMOs	F^{th} (au)	$-F^{th}$ (au)	$F^{th}_{\perp}$ (au)
methane	no crossing			
fluoromethane	no crossing			
formaldehyde	L + 1 ↔ L	0.040	0.017	
ethylene	L + 1 ↔ L	0.005		
acetylene	no crossing			
benzene	L + 2 ↔ L + 1, L	0.003		0.015
fluorobenzene	L + 2 ↔ L	0.008	0.005	0.020
chlorobenzene	L + 4 ↔ L + 1, L	0.007		
	L + 2 ↔ L + 1, L		0.005	
	L + 1 ↔ L			0.013
1,4-chlorobenzene	L + 4 ↔ L	0.009		
	L + 2 ↔ L	0.009		
	L + 1 ↔ L			0.018
hexafluorobenzene	no crossing			
pyridine	L + 2 ↔ L	0.012	0.007	

[a] $-F^{th}$ and $F^{th}_{\perp}$ denote the threshold fields for the reverse and transverse fields. L = LUMO.

TABLE 8: HOMO−LUMO Energy Gap (_HL) for Aliphatic Molecules at Various Field Strengths[a]

	CH_4		CH_3F		C_2H_4			HCHO		H_2C_2	
field (au)	Δ_{HL} (hartree)	$\Delta_{HL}{}^b$ (hartree)	Δ_{HL} (hartree)	$\Delta_{HL}{}^b$ (hartree)	Δ_{HL} (hartree)	$\Delta^{\perp}{}_{HL}$ (hartree)	$\Delta_{HL}{}^b$ (hartree)	Δ_{HL} (hartree)	$\Delta_{HL}{}^b$ (hartree)	Δ_{HL} (hartree)	$\Delta_{HL}{}^b$ (hartree)
0.030	0.248	0.494	0.329	0.568	0.154	0.228	0.292	0.225	0.473	0.135	0.272
0.020	0.308	0.532	0.345	0.582	0.204	0.254	0.342	0.222	0.493	0.197	0.336
0.010	0.362	0.565	0.355	0.588	0.250	0.267	0.389	0.220	0.502	0.256	0.398
0	0.390	0.587	0.348	0.573	0.271		0.462	0.217	0.483	0.305	0.454
−0.01 0	0.371	0.550	0.316	0.541				0.214	0.444		
−0.02 0	0.338	0.492	0.277	0.502				0.200	0.401		
−0.03 0	0.301	0.432	0.235	0.462				0.159	0.358		

[a] In methane, field is applied from C to H, along the C═C bond in ethylene, and along C≡C in acetylene. For the polar molecules, fields are applied along the permanent dipole moments. Values in the middle column correspond to the field applied perpendicular to the plane of ethylene. 1 hartree = 27.2116 eV. [b] HOMO−LUMO gap at MP2/6-311++G(2d,2p) (single point calculation; see text for detail) level of theory.

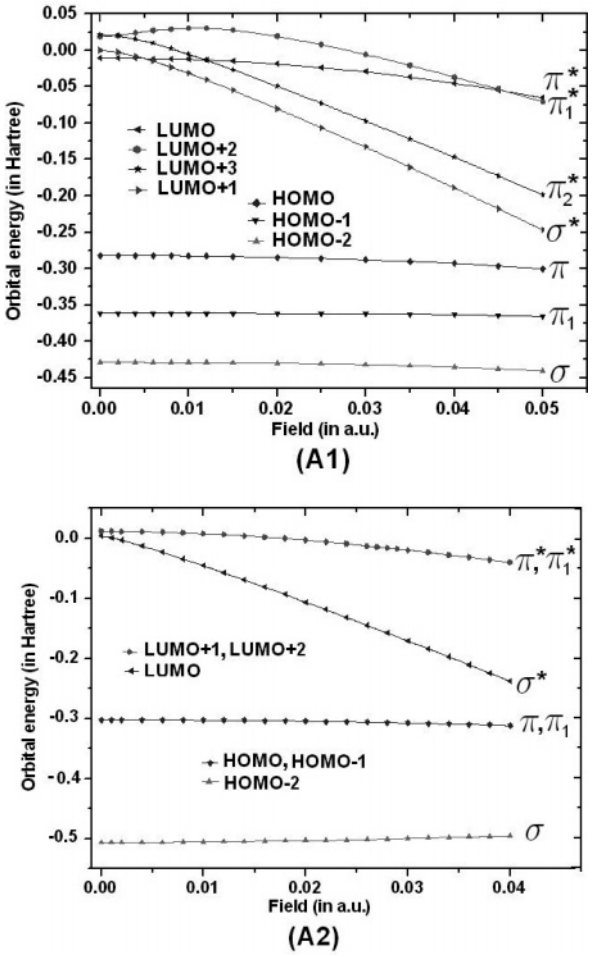

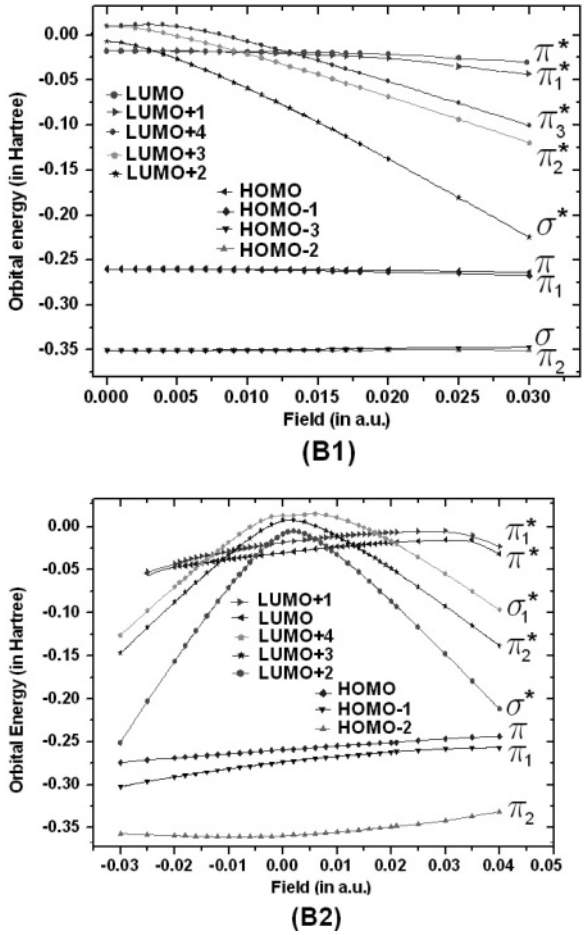

Figure 3. Variation of frontier orbital energies in ethylene (A1) and acetylene (A2) as the function of fields applied along the C−C bonds. (Labeling of MOs pertains to field-free case everywhere.)

Figure 4. Variation of frontier orbital energies in benzene (B1) and fluorobenzene (B2) with fields parallel to C−H and C−F bonds, respectively.

intensity exhibits a peak. Thus, a "tradeoff" between these vibrational modes is observed.

3. MO and MO-Energy Redistributions. The externally imposed electric field brings in a drastic redistribution of orbitals, an effect that hinges on the response of the electron density. We denote the LUMOs summarily by an asterisk (∗). Further, the symbols σ, π, σ^*, and π^* are essentially construed to be *notional* and depend only on the lobes and nodal surfaces, i.e., retention or alteration in the algebraic sign of the lobes of the orbital. In methane, HOMO, HOMO-1, and HOMO-2 and LUMO + 1, LUMO + 2, and LUMO + 3 are degenerate. With the increase in the field strength in the direction from C to H, the HOMO − 1, HOMO − 2 and LUMO + 1, LUMO + 2 pairs continue to remain degenerate with a steady decrease in the MO energy of σ^* LUMO. When the field is applied in opposite direction, the HOMO, HOMO − 1 and LUMO + 2, LUMO + 3 pairs preserve their degeneracy. The LUMO energy, on the contrary, once again decreases continuously. A similar trend has been noticed for the LUMO energy of fluoromethane. A decrease in LUMO energy for the field in the direction F to C (i.e., in the direction of its permanent dipole moment) is rather gradual. However, the energy of frontier HOMOs varies fairly linearly with field over a wide range. The higher LUMOs in these molecules are never seen to cross the LUMO (not depicted here), within the field range −0.050 through 0.040 au. HOMO−LUMO energy gap behavior for different applied field strengths has been presented in Table 8. The prediction of energy gap at

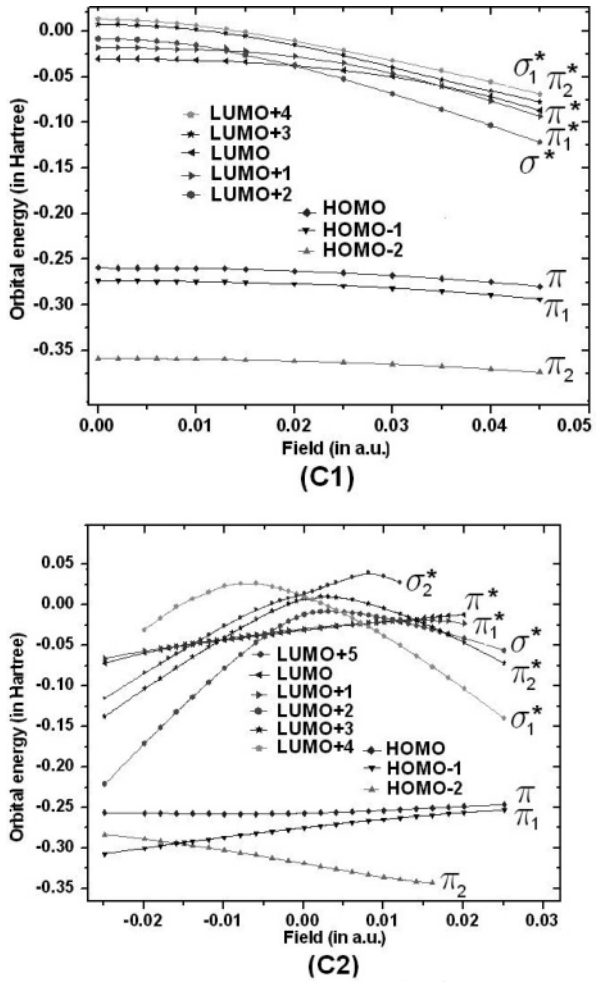

Figure 5. Variation in energies of MOs in fluorobenzene (C1) and chlorobenzene (C2) in response to the fields applied perpendicular to the molecular plane of fluorobenzene and along the permanent dipole moment of chlorobenzene.

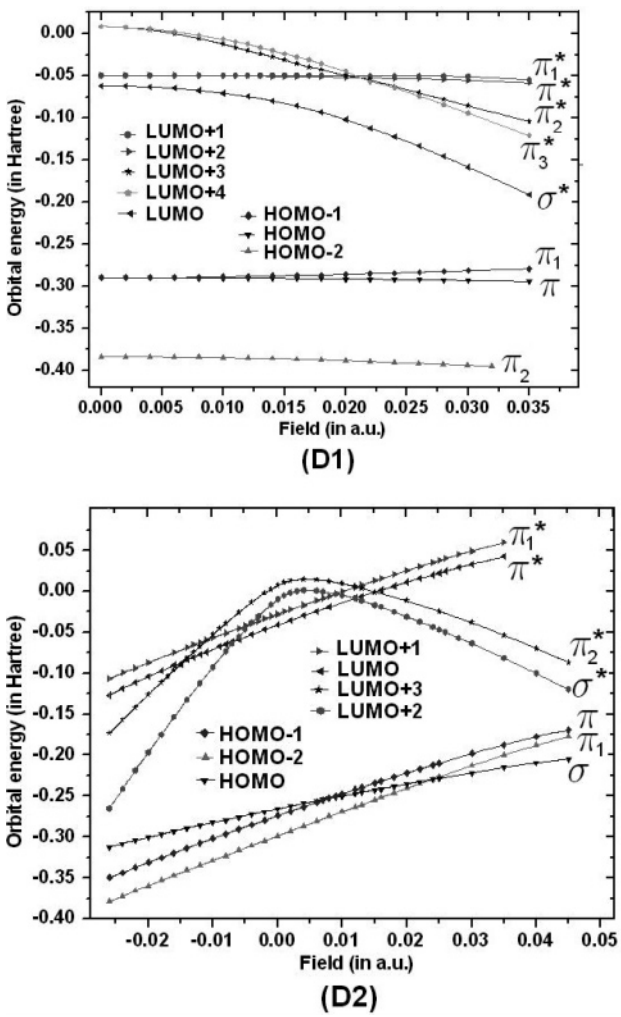

Figure 6. Variation of frontier orbital energies in hexafluorobenzene (D1) and pyridine (D2) with fields applied along along C−F bond in the case in hexafluorobenzene and along the permanent dipole moment of pyridine.

MP2/6-311++G(2d,2p) level is obtained by performing single point energy calculation on the geometry optimized at the B3LYP/6-311++G(2d,2p) level of theory. Increasing field in the direction of permanent dipole moment of formaldehyde lowers the energy of delocalized σ^* LUMO + 1 while the energy of π^* LUMO increases almost linearly. The energies of HOMOs remain practically unchanged. At the field strength of 0.040 au, a role reversal is observed: the energy of LUMO + 1 gets lowered below that of LUMO and thus becomes the actual LUMO. Above this threshold, the LUMO energy and hence the HOMO−LUMO energy gap decreases rapidly. Reverse is the case while applying field in the opposite direction. Variation in MO energies of ethylene and acetylene is displayed in Figure 3. The threshold field in ethylene for LUMO + 1 ⇔ LUMO crossover is 0.005 au (Table 7).

Figure 4 depicts variation in the energies of MOs of benzene and fluorobenzene for field applied in the molecular planes. Interchange of degenerate MOs in benzene, viz., LUMO and LUMO + 1 and HOMO − 2 and HOMO − 3 takes place at respective field strengths, 0.002 and 0.003 au (cf. Figure 7). Evolution of MOs of fluorobenzene with applied field is presented later in Figure 8. Meanwhile, Figure 5 portrays variation in energies of MOs of fluorbenzene as a function transverse field. Crossing of higher LUMOs with the first LUMO and the corresponding threshold fields are displayed in Table 7. Variation of MO energies in 1,4-chlorofluorobenzene in response to the applied field is similar to that shown for chlorobenzene of Figure 5, except that the π^* LUMO and LUMO + 1 orbital energies in 1,4-chlorofluorobenzene are separated by 0.012 hartree. The field applied perpendicular to the plane of the molecules is essentially seen to have similar effects on benzene and fluorobenzene, whereas in chlorobenzene the degenerate LUMO and LUMO + 1 get interchanged at the field strength of 0.013 au, beyond which the LUMO energy and hence the HOMO−LUMO energy gap decreases. It is noteworthy that Hartree−Fock (HF) theory overestimates the HOMO−LUMO energy gap (since the LUMO energy at the HF level is too high[31]) whereas DFT underestimates the gap,[32] as an artifact of the approximate exchange-correlation prescriptions. It may be remarked that the so termed GW-approximation[33] yields the field-free energy gap of benzene to be 10.51 eV, which compares well with the HF value of 10.34 eV, whereas B3LYP estimates it to be 6.58 eV.

In hexafluorobenzene, the field is applied along a C−F bond. In its absence, LUMO + 1/LUMO + 2, LUMO + 3/LUMO + 4, HOMO/HOMO − 1, and some other inner HOMO pairs are degenerate. On increasing the field, degeneracy of the frontier MOs gets lifted. The energy of σ^* LUMO decreases continuously while energies of π^* LUMO + 1 and LUMO + 2 remain fairly unaffected until the applied field reaches high values ∼0.025 au (cf. Figure 6). As in methane, fluoromethane, and

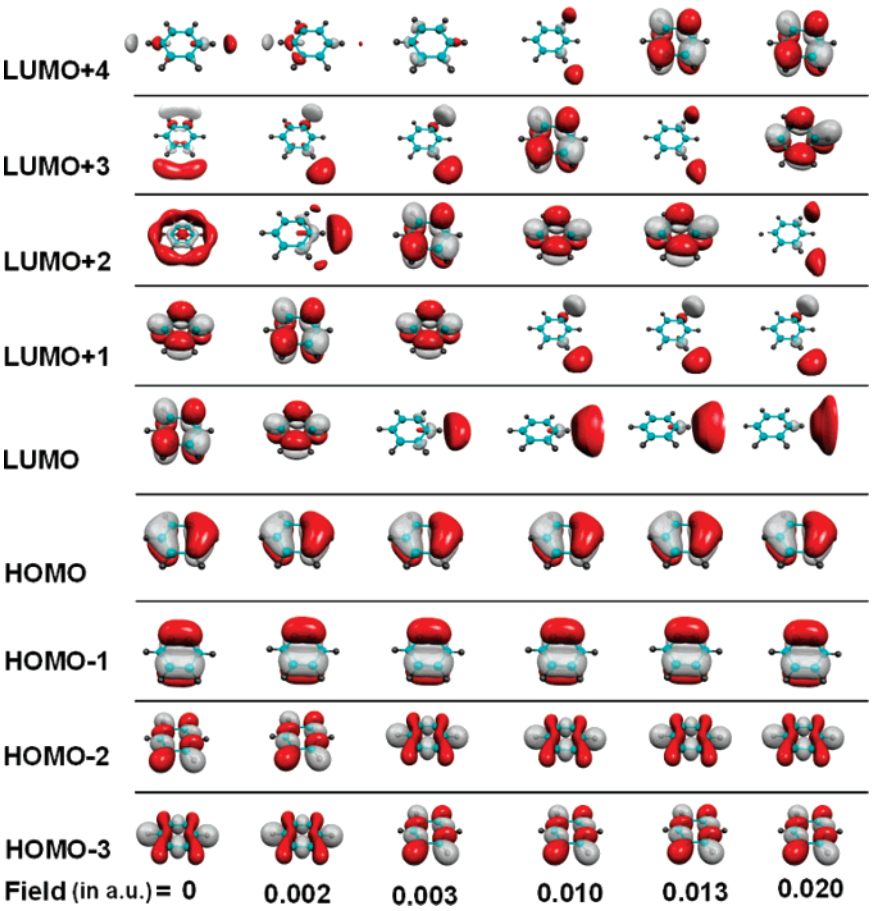

Figure 7. Evolution of frontier MOs of benzene as a function of field applied along the C−H bond. Orbitals are drawn at the contour value ±0.03 au.

TABLE 9: HOMO−LUMO (HL) Energy Gap of Aromatic Molecules at Various Field Strengths[a]

	C_6H_6				C_6H_5F			C_6H_5Cl		1,4-C_6H_4ClF		C_6F_6		C_5H_5N
field (au)	Δ_{HL} (hartree)	Δ_{HL}[b] (hartree)	Δ_{HL}[c] (hartree)	$\Delta^{\perp}_{HL}$ (hartree)	Δ_{HL} (hartree)	Δ_{HL}[c] (hartree)	$\Delta^{\perp}_{HL}$ (hartree)	Δ_{HL} (hartree)	$\Delta^{\perp}_{HL}$ (hartree)	Δ_{HL} (hartree)	$\Delta^{\perp}_{HL}$ (hartree)	Δ_{HL} (hartree)	$\Delta^{\perp}_{HL}$ (hartree)	Δ_{HL} (hartree)
0.040		0.055		0.180	0.031[d]	0.149	0.171		0.149		0.142		0.167	0.077
0.030	0.038[d]	0.143	0.140	0.206	0.098	0.216	0.199	0.065	0.181	0.046	0.176	0.122	0.193	0.134
0.020	0.123	0.229	0.227	0.230	0.164	0.282	0.225	0.144	0.211	0.131	0.207	0.183	0.213	0.190
0.010	0.201	0.312	0.310	0.241	0.222	0.343	0.228	0.215	0.224	0.207	0.213	0.218	0.224	0.233
0	0.242	0.380	0.377		0.229	0.381		0.225		0.213		0.227		0.224
−0.010					0.192			0.179		0.202				0.190
−0.020					0.112			0.086		0.126				0.103
−0.030					0.023[d]					0.042				0.019

[a] In benzene and hexafluorobenzene fields are applied along the C−H and C−F bond, respectively, whereas, in polar molecules, fields are applied along the permanent dipole moments. HL's without superscript are the B3LYP/6-311++G(2d,2p) values. Values in the last column are HL's corresponding to a field applied perpendicular to the plane of the molecules. [b] HOMO−LUMO gap at the RHF/6-311++G(2d,2p) level of theory. [c] HOMO−LUMO gap at the MP2/6-311++G(2d,2p) (single point calculation; see text for detail) level of theory. [d] Value corresponding to the transition state structure. See ref 33 for benzene HOMO−LUMO gaps in the gas phase and crystal phase and adsorbed on the graphite surface (flat and perpendicular).

acetylene, hexafluorobenzene is devoid of a threshold field, beyond which HOMO−LUMO gap would decrease significantly (Table 9). In pyridine, the field is applied in the direction of permanent dipole moment (directed in the direction N → C−H). Variation in the MO energies of pyridine with field is pictured in Figure 6.

As remarked earlier, the planar aromatic species retain their planarity for the applied electric fields in the plane along or opposite to the dipole moment. On the other hand, fields perpendicular to the plane do distort the molecular plane, rendering the structure convex toward the applied electric field, except for hexafluorobenzene, which becomes concave due to electronegative fluorine atoms. For this molecule, although the degeneracy of frontier HOMOs gets lifted by the applied field, the inner MOs still remain degenerate even at moderately high fields. This behavior may attributed from the response of the lone pairs contributed by the fluorine atoms.

To gauge the influence of the imposed field on the electronic excitation involving transition from frontier HOMOs → LUMOs, some typical time-dependent density functional theory (TD−DFT) calculations were carried out at the same basis set [6-311++G(2d,2p)]. It is observed (cf. Tables 10 and 11) that the transitions involving (π, π^*) MOs are far more intense than those involving (π, σ^*) (not shown). In acetylene, the excitation consisting of $\pi \rightarrow \pi^*_1$, $\pi_1 \rightarrow \pi^*$ transitions is favored at lower fields but, at higher fields, $\pi \rightarrow \pi^*$, $\pi_1 \rightarrow \pi^*_1$ transitions lead

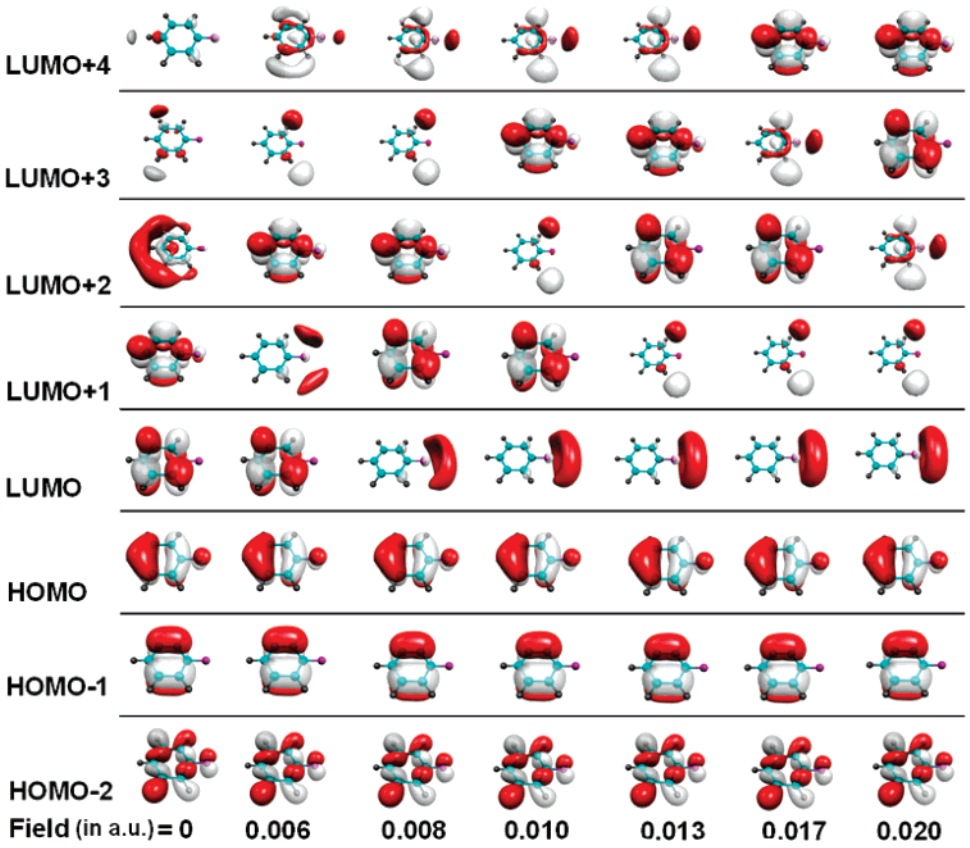

Figure 8. Depiction at a glance of the variation of frontier MOs of fluorobenzene as a function of field applied parallel to its permanent dipole moment. The same contour value of ±0.03 au is used.

TABLE 10: Electronic Excitation Energies and Corresponding Oscillator Strengths (au) Calculated by TD−DFT [B3LYP/6-311++G(2d,2p)] for the Most Intense Electronic Transitions (HOMOs → LUMOs) Involving Frontier MOs[a]

molecule	field (au)	transition composition (frontier MOs)	excitation energy (nm^{-1})	oscillator strength
ethylene	0	T	165.8	0.0745
	0.005	T	166.5	0.0718
	0.010	T	168.5	0.0646
	0.020	T	176.0	0.0439
		T	145.2	0.0435
acetylene	0	S	136.0	0.1315
	0.005	S	138.2	0.0996
	0.010	S	142.2	0.0758
		S	125.0	0.0713
	0.020	R	118.9	0.0850

[a] Other accompanying transitions to higher LUMOs leading to excited states are not shown. Field is applied parallel to the C−C bond: T = $\pi \rightarrow \pi^*$; S = $\pi \rightarrow \pi_1^*$, $\pi_1 \rightarrow \pi^*$; R = $\pi \rightarrow \pi^*$, $\pi_1 \rightarrow \pi_1^*$. (For notional notation, see text for details.)

TABLE 11: Electronic Excitation Energies Calculated from TD−DFT [B3LYP/6-311++G(2d,2p)][a]

molecule	field (au)	transition composition (frontier MOs)	excitation energy (nm^{-1})	oscillator strength
benzene	0	A	178.3	0.1205
		B	178.3	0.1205
	0.005	A	178.5	0.1199
		B	178.8	0.1193
	0.010	A	179.2	0.1182
		B	180.5	0.1141
	0.015	A	180.4	0.1081
		B	184.1	0.0948
	0.020	A	181.2	0.0976
		B	190.3	0.0608
fluorobenzene	0	A	178.4	0.5366
		B	178.0	0.5773
	0.005	A	178.0	0.1116
		B	177.3	0.1116
	0.010	A	178.2	0.1107
		B	177.1	0.1065
	0.015	A	179.1	0.1057
		B	177.5	0.0978
	0.020	A	181.1	0.0918
		B	176.8	0.0811

[a] Only the most intense electronic transition (HOMOs → LUMOs) involving frontier MOs are presented. Field is applied along the C−H bond in benzene and parallel to the permanent dipole moment in fluorobenzene: A = $\pi \rightarrow \pi^*$, $\pi_1 \rightarrow \pi_1^*$; B = $\pi \rightarrow \pi_1^*$, $\pi_1 \rightarrow \pi^*$. (For notional notation, see text for details.)

to an excited state. Tables 10 and 11 thus reveal that an increase in the applied field strength by and large increases the excitation energies corresponding to significant electronic transitions among frontier MOs with a concomitant decrease in their oscillator strengths.

At this juncture, it is worthwhile to mention that TD−DFT could admittedly lead to erroneous results[34] in the case where substantial bond stretching occurs in the excited state during the excitation process. The excitation energies reported in Tables 10 and 11 are well below the fields that drastically change the geometry of molecules, causing them to dissociate.

IV. Concluding Remarks

Systematic investigations on the response of molecules to an externally imposed electric field have been presented. The changes in the structure, vibrational frequencies, and energy spectrum of MOs have been analyzed. For aromatic molecular

systems, the field applied in the plane of molecules influence significantly the MOs more than when applied perpendicular to the aromatic ring. In contrast, the fields perpendicular to the aromatic ring distort the planarity of the aromatic ring. The shifts in the stretching frequency (vibrational Stark effect) of fluorobenzene is quite significant, in conjunction with the Stark tuning rate having an appreciable value of $\cong 0.73$ cm^{-1}/(MV/cm). This suggests that the F−C bond stretch in fluorobenzene could serve as a probe to estimate local electric field strengths at specific sites of molecular complexes as is the case for C−O, C−N, and N−O bonds.[18,29] For molecules having a π-type antibonding LUMO (e.g., ethylene, benzene, fluorobenzene, etc.), there exists a threshold field above which the HOMO−LUMO gap decreases rapidly. This is attributed to the delocalized σ* LUMOs which are more susceptible to polarization (than the localized π-type antibonding LUMO); hence, their energy gets lowered even below that of the LUMO, resulting into a reduction in the HOMO−LUMO energy gap or, equivalently, in absolute hardness, $\tau = (E_{LUMO} - E_{HOMO})/2$—a measure of stability of molecules. TD−DFT calculations reveal that the transitions involving (π, π*) MOs are far more intense than those involving (π, σ*). These investigations on various properties of isolated molecules in external electric fields are hoped to be useful in understanding the characteristics of organic molecules use in molecular electronics. Further, it would be of great interest to investigate the interaction of molecular clusters with external fields, and investigations on these lines are underway.

Acknowledgment. D.R. gratefully acknowledges support from Human Resource Development Department, Government of Sikkim, Gangtok, India. R.K.P. is thankful for the financial support from The University Grants Commission (UGC), New Delhi, India, disbursed through PHY/RG9 to The University of Pune, Pune, India, and to a visiting professor position at Tulane University, New Orleans, LA. S.P.G. also wishes to acknowledge financial support from the UGC (Research Project F 30-72/2004 (SR)).

References and Notes

(1) Choi, Y. C.; Kim, W. Y.; Park, K.-S.; Tarakeshwar, P.; Kim, K.-S. *J. Chem. Phys.* **2005**, *122*, 094706.

(2) Li, Y.; Zhao, J.; Yin, X.; Yin, G. *J. Phys. Chem. A* **2006**, *110*, 11130.

(3) (a) Tian, W.; Datta, S.; Hong, S.; Reifenberger, R.; Henderson, J. I.; Kubiak, C. P. *J. Chem. Phys.* **1998**, *109*, 2874. (b) Xue, Y.; Datta, S.; Ratner, M. A. *J. Chem. Phys*. **2001**, *115*, 4292. (c) Emberly, E. G.; Kirczenow, G. *Phys. Rev. Lett.* **2003**, *91*, 188301.

(4) Wang, C. K.; Fu, Y.; Luo, Y. *Phys. Chem. Chem. Phys*. **2001**, *3*, 5017.

(5) Tóbik, J.; Corso, A. D.; Scandolo, S.; Tosatti, E. *Surf. Sci.* **2004**, *566*, 644.

(6) (a) Nitzam, A.; Ratner, M. A. *Science* **2003**, *300*, 1384. (b) Remacle, F.; Levine, R. D. *Faraday Discuss*. **2006**, *131*, 45.

(7) (a) Aviram, A.; Ratner, M. A. *Chem. Phys. Lett*. **1974**, *29*, 277. (b) Aviram, A. *J. Am. Chem. Soc*. **1988**, *110*, 5687. (c) Brady, A. C.; Hodder, B.; Martin, A. S.; Sambles, J. R.; Ewels, C. P.; Jones, R.; Briddon, P. R.; Musa, A. M.; Panetta, C. A.; Mattern, D. L. *J. Mater. Chem.* **1999**, *9*, 2271. (d) Jiang, F.; Zhou, Y. X.; Chen, H.; Note, R.; Mizuseki, H.; Kawazoe, Y. *J. Chem. Phys.* **2006**, *125*, 084710.

(8) (a) Buckingham, A. D. *J. Chem. Phys*. **1959**, *30*, 1580. (b) McLean, A. D.; Yoshimine, M. J. *Chem. Phys*. **1967**, *47*, 1927.

(9) (a) Kern, C. W.; Matcha, R. L. *J. Chem. Phys*. **1968**, *49*, 2081. (b) Krohn, B. J.; Ermler, W. C.; Kern, C. W. *J. Chem. Phys*. **1974**, *60*, 22. (c) Pandey, P. K. K.; Santry, D. P. *J. Chem. Phys.* **1979**, *73*, 2899. (d) Bishop, D. M. *Rev. Mod. Phys*. **1990**, *62*, 343. (e) Martí, J.; Bishop, D. M. *J. Chem. Phys.* **1993**, *99*, 3860. (f) Luis, J. M.; Duran, M.; Andrés, J. L. *J. Chem. Phys*. **1997**, *107*, 1501.

(10) (a) Chottopadhyay, A.; Boxer, S. G. *J. Am. Chem. Soc*. **1995**, *117*, 1449. (b) Park, E. S.; Andrews, S. S.; Hu, R. B.; Boxer, S. G. *J. Phys. Chem. B* **1999**, *103*, 9813. (c) Phillips, G. N., Jr.; Teodoro, M. L.; Li, T.; Smith, B.; Olson, J. S. *J. Phys. Chem. B* **1999**, *103*, 8817. (d) Park, E. S.; Thomas, M. R.; Boxer, S. G. *J. Am. Chem. Soc*. **2000**, *122*, 12297. (e) Suydam, I. T.; Snow, C. D.; Pande, V. S.; Boxer, S. G. *Science* **2006**, *313*, 200.

(11) Bishop, D. M. *J. Chem. Phys*. **1993**, *98*, 3179.

(12) (a) Duran, M.; Andrés, J. L.; Lledós, A.; Bertrán, J. *J. Chem. Phys*. **1989**, *90*, 328. (b) Andrés, J. L.; Martí, J.; Duran, M.; Lledós, A.; Bertrán, J. *J. Chem. Phys*. **1991**, *95*, 3521. (c) Hermansson, K.; Tepper, H. *Mol. Phys*. **1996**, *89*, 1291. (d) Reimers, J. R.; Hush, N. S. *J. Chem. Phys. A* **1999**, *103*, 10580. (e) Martí, J.; Luis, J. M.; Duran, M. *Mol. Phys.* **2000**, *98*, 513. (f) Andrews, S. S.; Boxer, S. G. *J. Phys. Chem. A* **2002**, *106*, 468. (e) Dalosto, S. D.; Vanderkooi, J. M.; Sharp, K. A. *J. Phys. Chem. B* **2004**, *108*, 6450.

(13) Masunov, A.; Dannenberg, J. J.; Contreras, R. H. *J. Phys. Chem. A* **2001**, *105*, 4737.

(14) (a) Pacchioni, G.; Bagus, P. S. *Phys. Rev. B* **1989**, *40*, 6003. (b) Hernández, M. G.; Curulla, D.; Clotet, A.; lllas, F. *J. Chem. Phys*. **2000**, *113*, 364. (c) Manca, C.; Allouche, A. *J. Chem. Phys*. **2001**, *114*, 4226.

(15) Lambert, D. K. *J. Vac. Sci. Technol., B* **1985**, *3*, 1479.

(16) (a) Lambert, D. K. *Phys. Rev. Lett*. **1983**, *50*, 2106. (b) Andrews, S. S.; Boxer, S. G. *J. Phys. Chem. A* **2000**, *104*, 11853.

(17) (a) Martí, J.; Bishop, D. M. *J. Chem. Phys.* **1993**, *99*, 3860. (b) Hermansson, K. *J. Chem. Phys*. **1993**, *99*, 861. (c) Brewer, S. H.; Franzen, S. *J. Chem. Phys*. **2003**, *119*, 851.

(18) (a) Lehle, H.; Kriegl, J. M.; Nienhaus, K.; Deng, P.; Fengler, S.; Nienhaus, G. U. *Biophys. J*. **2005**, *88*, 1978. (b) Fafarman, A. T.; Webb, L. J.; Chuang, J. I.; Boxer, S. G. *J. Am. Chem. Soc*. **2006**, *128*, 13356.

(19) (a) Whittle, E.; Dows, D. A.; Pimentel, G. C. *J. Chem. Phys*. **1954**, *22*, 1943. (b) Becker, E. D.; Pimentel, G. C. *J. Chem. Phys*. **1956**, *25*, 224.

(20) (a) Parker, J. K.; Davis, S. R. *J. Am. Chem. Soc*. **1999**, *121*, 4271. (b) Chillier, X.; Boulet, P.; Chermette, H.; Salama, F.; Weber, J. *J. Chem. Phys*. **2001**, *115*, 1769. (c) Sundararajan, K.; Sankaran, K.; Viswanathan, K. S.; Kulkarni, A. D.; Gadre, S. R. *J. Phys. Chem. A* **2002**, *106*, 1504. (d) Engdahl, A.; Karlström, G.; Nelander, B. *J. Chem. Phys*. **2003**, *118*, 7797.

(21) Frisch, M. J.; Trucks, G. W.; Schlegel, H. B.; Scuseria, G. E.; Robb, M. A.; Cheeseman, J. R.; Montgomery, J. A., Jr.; Vreven, T.; Kudin, K. N.; Burant, J. C.; Millam, J. M.; Iyengar, S. S.; Tomasi, J.; Barone, V.; Mennucci, B.; Cossi, M.; Scalmani, G.; Rega, N.; Petersson, G. A.; Nakatsuji, H.; Hada, M.; Ehara, M.; Toyota, K.; Fukuda, R.; Hasegawa, J.; Ishida, M.; Nakajima, T.; Honda, Y.; Kitao, O.; Nakai, H.; Klene, M.; Li, X.; Knox, J. E.; Hratchian, H. P.; Cross, J. B.; Bakken, V.; Adamo, C.; Jaramillo, J.; Gomperts, R.; Stratmann, R. E.; Yazyev, O.; Austin, A. J.; Cammi, R.; Pomelli, C.; Ochterski, J. W.; Ayala, P. Y.; Morokuma, K.; Voth, G. A.; Salvador, P.; Dannenberg, J. J.; Zakrzewski, V. G.; Dapprich, S.; Daniels, A. D.; Strain, M. C.; Farkas, O.; Malick, D. K.; Rabuck, A. D.; Raghavachari, K.; Foresman, J. B.; Ortiz, J. V.; Cui, Q.; Baboul, A. G.; Clifford, S.; Cioslowski, J.; Stefanov, B. B.; Liu, G.; Liashenko, A.; Piskorz, P.; Komaromi, I.; Martin, R. L.; Fox, D. J.; Keith, T.; Al-Laham, M. A.; Peng, C. Y.; Nanayakkara, A.; Challacombe, M.; Gill, P. M. W.; Johnson, B.; Chen, W.; Wong, M. W.; Gonzalez, C.; Pople, J. A. *Gaussian 03*, revision C.02; Gaussian, Inc.: Wallingford, CT, 2004.

(22) Deleuze, M. S.; Trofimov, A. B.; Cederbaum, L. S. *J. Chem. Phys*. **2001**, *115*, 5859.

(23) Khan, R.; Lara, E. C. D.; Möller, K. D. *J. Chem. Phys*. **1985**, *83*, 2653.

(24) Becke, A. D. *J. Chem. Phys.* **1993**, *98*, 5648.

(25) Lee, C.; Yang, W.; Parr, R. G. *Phys. Rev. B* **1988**, *37*, 785.

(26) Lara, E. C. D.; Khan, R.; Seloudoux, R. *J. Chem. Phys*. **1985**, *83*, 2646.

(27) Kriegl, J. M.; Neinhans, K.; Deng, P.; Fuchs, J.; Neinhaus, G. U. *Proc. Natl. Acad. Sci. U.S.A.* **2003**, *100*, 7069.

(28) Tóbik, J.; Corso, A. D. *J. Chem. Phys*. **2004**, *120*, 9934.

(29) Suydam, I. T.; Boxer, S. G. *Biochemistry* **2003**, *42*, 12050.

(30) (a) Dreuw, A.; Head-Gordon, M. *Chem. Rev.* **2005**, *105*, 4009. (b) Hessler, P.; Park, J.; Burke, K. *Phys. Rev. Lett.* **1999**, *82*, 378. (c) Ullrich, C. A.; Burke, K. *J. Chem. Phys.* **2004**, *121*, 28. (d) Petersilka, M.; Gross, E. K. U.; Burke, K. *Int. J. Quantum. Chem.* **2000**, *80*, 534.

(31) Szabo, A.; Ostlund, N. S. *Modern Quantum Chemistry: Introduction to Advanced Electronic Structure Theory*; Dover Publications, Inc.: Mineola, NY, 1996.

(32) Burke, K.; Gross, E. K. U. *Density Functionals: Theory and Applications*; Joubert, D., Ed.; Springer: Berlin, 1998.

(33) Neaton, J. B.; Hybertsen, M. S.; Louie, S. G. *Phys. Rev. Lett*. **2006**, *97*, 216405.

(34) Cai, Z.-L.; Reimers, J. R. *J. Chem. Phys*. **2000**, *112*, 527.